

**Fermi National Accelerator Laboratory**

**FERMILAB-FN-589**

# **Hadronic and Electromagnetic Transverse Calorimetric Segmentation**

W. Wu, A. Beretvas, D. Green and J. Marraffino

*Fermi National Accelerator Laboratory  
P.O. Box 500, Batavia, Illinois 60510*

April 1992

## **Disclaimer**

*This report was prepared as an account of work sponsored by an agency of the United States Government. Neither the United States Government nor any agency thereof, nor any of their employees, makes any warranty, express or implied, or assumes any legal liability or responsibility for the accuracy, completeness, or usefulness of any information, apparatus, product, or process disclosed, or represents that its use would not infringe privately owned rights. Reference herein to any specific commercial product, process, or service by trade name, trademark, manufacturer, or otherwise, does not necessarily constitute or imply its endorsement, recommendation, or favoring by the United States Government or any agency thereof. The views and opinions of authors expressed herein do not necessarily state or reflect those of the United States Government or any agency thereof.*

# HADRONIC AND ELECTROMAGNETIC TRANSVERSE CALORIMETRIC SEGMENTATION

W. Wu, A. Beretvas, D. Green, J. Marraffino

Fermi National Accelerator Laboratory  
Batavia, IL 60510

## 1.0 INTRODUCTION

In a calorimeter system, one of the major cost drivers is the number of towers. The longitudinal segmentation of the calorimeter system is driven by a need for  $e$  identification, a need for monitoring of radiation damage, and a need for monitoring and control of hadronic energy leakage [1]. The transverse segmentation of the system mirrors the characteristic sizes of the shower processes; the Moliere radius for the electromagnetic (EM) compartment and the absorption length for the hadronic (HAD) compartment. A summary of the requirements has already been given in the SDC calorimeter Conceptual Design Report (CDR). [2] In this note we present additional refinements which have been made since that time, or details which are not available in that document.

## 2.0 DIJET MASS RESOLUTION

The dijet (JJ) mass resolution was the subject of an intensive study at the time of the SDC LoI. [3] Since that time, the mass range has been extended to cover 10 TeV dijet masses. In addition, a systematic study of the effect of calorimeter transverse segmentation has been made. A plot of the mass resolution for low Pt  $Z \rightarrow JJ$  decays, high Pt  $Z$  decays, and low Pt 10 TeV  $Z'$  decays is shown in Fig. 1. Clearly, for tower sizes  $< 0.1$ , the effect of the tower size on the mass resolution is minimal. Note that the actual hadronic shower is taken to be of zero transverse size in this plot. A simplified model of dijets, ignoring fragmentation, leads to a mass resolution,  $dM$ , for dijet mass  $M$ , due to angular error  $d(\theta)$

$$dM/M = d(\theta) [Pt/M] \quad (1)$$

Clearly, only highly boosted light dijets will have a significant contribution due to any angular error in comparison to the energy error due to the calorimeter measurement,  $dM/M = [dP/P] / \sqrt{2}$ . This expectation is borne out in Fig. 1; only the highly boosted  $Z$  show a substantial effect due to segmentation.

## 3.0 HADRONIC SHOWER SIZE

Any segmentation effect can be expected to be somewhat washed out when the finite size due to the hadronic shower is added to the model. In Fig. 2 is shown the radial distribution of hadronic shower energy in the parametrization of Ref. 4. Since, at 90 degrees,  $d(\theta) = d(\eta) = dz/R$  and  $R \sim 2$  meters, the mean shower size,  $dz = 2(7.5 \text{ cm})$ , covers a range in  $\eta$  of 0.075. Therefore, we expect that the effect of segmentation will be washed out by the

finite shower size for tower size  $< 0.075$ . Confirmation of that expectation is shown in Fig. 3, which shows Z dijet masses for EM segmentation of 0.05 and HAD segmentation of 0.05 and 0.1. The insensitivity of dM to segmentation has also been observed in other studies. [5]

#### 4.0 THE DECAY CHAIN $t \rightarrow W + b \rightarrow c + e + \nu$

In order to study EM segmentation, it was decided to look at a process which yields electrons near jets. Top pairs with a top mass = 150 GeV were generated. The decay mode of the W was unconstrained while the b quark was forced to make a semileptonic decay. In general, no cut on Pt of the lepton with respect to the c jet axis was made. Therefore, the e which are studied are not forced to be isolated. The pseudorapidity distribution of the electrons is shown in Fig. 4. The electrons clearly are spread over the full 6 units of rapidity spanned by the SDC central calorimetry. Figure 5 shows the Pt distribution of the electrons. The mean value is only 10.5 GeV. The  $\sim 75$  GeV acquired from the 2 body top decay to W+b is washed out by the 3 body semileptonic decay. Again, this sample is deemed to be representative of the difficult category of electrons which are not isolated.

#### 5.0 EM/HAD and HAD SEGMENTATION

The EM segmentation was chosen to be 0.05 for a variety of reasons. One of them was that for this segmentation the EM/HAD ratio for the electrons was  $\sim 50$  [2]. This value was compatible with the cuts available to SDC triggers at low luminosity. Smaller segmentation, of the size of the natural scale of e showers, is not economically feasible. That scale is only realized by the shower maximum (SM) strips, as is discussed later. The choice of 0.05 EM segmentation means that leakage of  $> 2\%$  into the HAD compartment cannot be tolerated or the EM/HAD ratio cut would be degraded. The EM depth must be sufficient to insure low leakage up to the highest energies desired for study in SDC.

Fixing the EM segmentation at 0.05, one can ask what effect the HAD segmentation has on the EM/HAD ratio. In Fig. 6 the functional dependence of the EM/HAD ratio on the radius R of a cone, defined to be  $R = \sqrt{(\Delta\eta)^2 + (\Delta\phi)^2}$ , centered on the EM centroid tower is given. Note that all the energy in a tower is assumed to reside at the tower center. If a tower center falls within the cone, all its energy is taken to fall within that cone. Clearly, the coarser HAD segmentation leads to a reduction in the EM/HAD ratio. At a cone size of  $R = 0.1$ , the reduction of the ratio is quite small as HAD segmentation goes from 0.05 to 0.1. A typical LEGO plot for EM plus HAD is shown in Fig. 7 for pixel sizes of 0.05. Some idea of the "ambient" background to the LEGO plot in the vicinity of the e can be obtained from an examination of this plot. It seems that, even in the nonisolated environment chosen, a small HAD segmentation is not crucial to obtaining a large value of EM/HAD.

#### 6.0 HIGH LUMINOSITY PILEUP

A segmentation which yields acceptable performance at design luminosity may degrade at a luminosity 10 times higher. To study pileup

effects, minbias events were overlaid on the top events. The number distribution was a Poisson distribution with a mean of 15. This value for the mean is that expected for operation at 10 times the SSC design luminosity or  $10^{34}/(\text{cm}^2\text{-sec})$ . A typical LEGO plot is given in Fig. 8. Direct comparison with Fig. 7 allows one to get some idea as to the severity of the pileup problem. Shown in Fig 9 is a plot similar to that of Fig. 6 except that the EM segmentation is fixed at 0.05 and the HAD is fixed at 0.1. The 2 sets of data points correspond to top events alone and top events with an average of 15 minbias events overlapped. The pileup effects clearly increase with R. At  $R=0.1$  the pileup reduction in the EM/HAD ratio is  $\sim 30\%$ . Given that the mean pileup can be subtracted, the fluctuations in the pileup lead to a smaller,  $\sim 15\%$ , effect. The conclusion derived from this study was that 0.1 HAD segmentation does not lead to unacceptable pileup effects for this physics process.

## 7.0 SHOWER MAXIMUM STRIP LENGTH

The same top events were used in a study of the shower maximum (SM) detector. This detector was taken to have crossed strips of width =  $0.05/8=0.00625$ . For a radius of 2 m, this corresponds to a physical size of 1.25 cm. This size is comparable to the Moliere radius in Pb. This detector is the only SDC calorimeter element with a level of granularity comparable to the natural transverse EM shower size. Naturally, the question arises as to how long the strips can be made.

That question was studied by modifying the LEGO plots to be asymmetric. The tracking centroid was taken to be the impact of the e trajectory on the front face of the EM calorimeter compartment. The SM centroid was taken to be the energy weighted center of gravity of the 3 strips nearest the impact point. The e energy was distributed transversely according to a 2 component exponential parametrization which attempts to model a hot core and the cool low energy shower components. [6] Note that no fluctuations in the EM shower transverse development are implemented in the model. Given that the test beam results show resolutions of  $\sim 2\text{mm}$  [7], or 0.001, it is clear that pileup effects are small for all the studies done here.

The results for the SM/track match for both " $\eta$ " and " $\phi$ " strips are shown in Fig. 10. The mean deviation of the match as a function of the strip length is shown. No pileup is applied for the full curves, while a mean of 15 minbias events is overlapped with the  $\bar{t}\bar{t}$  events for the dashed curves. Note that for strip widths  $< 0.2$ , the pileup fluctuations at low and high luminosity are less than 1 mm ( $\sim 0.0005$ ). Note also that high luminosity operation makes little impact on the SM performance for strip widths  $< 0.2$ .

To give an idea of the sweeping effect of the magnetic field for these nonisolated  $\bar{t}\bar{t}$  events, in Fig. 11 is shown the LEGO plot of the EM plus HAD compartments with high luminosity conditions and with the B field off. A direct comparison with Fig. 8, which is the same plot with the B field on, shows the sweeping effect clearly. Ultimately, however, the adverse effect on the centroid match to the e track is small.

The dependence of the mean deviation of the match of SM/tracking is rather weakly dependent on the SM strip length. This is not unexpected. The

fluctuations in the overlap of tracks from the underlying event should go as the square root of the strip area, or the square root of the strip length at fixed width. The pileup energy itself scales as the strip length. The shape of the curves shown in Fig. 10 are consistent with this weak type of functional dependence.

The conclusion of this study was that the SM strip length could be made 0.2 even for the case of boosted b jets and still not suffer from background fluctuations due to fluctuations in the underlying event. Clearly, at higher luminosity, the strips should be shorter. One expects that the pileup error should scale as the square root of the luminosity increase. Therefore, SDC plans to have the ability to electronically reduce the SM strip length to the physical length 0.05 at the highest luminosity if necessary.

## 8.0 SUMMARY

Several physical processes have been studied in an attempt to quantitatively assess the need for transverse segmentation in SSC calorimetry. The HAD segmentation does not effect dijet masses, even when the jets are highly boosted if the HAD segmentation is  $\leq 0.1$ . This occurs because of the basic limitation on jet measurement due to hadronic shower size.

Electron segmentation was studied by looking at a difficult process, e within the region of boosted b jets having c jet fragments. No isolating Pt cut was imposed on the electrons in question in order to see how stringent the basic process makes the requirements. The EM segmentation of 0.05 was chosen to insure that a EM/HAD cut in the trigger would not be biasing. With EM(HAD) segmentation of 0.05(0.1), within  $R = 0.05$  (about 1 HAD tower), a cut of EM/HAD  $> 30$  is efficient for this process. This conclusion is not changed for luminosities of up to  $10^{34}/(\text{cm}^2 \cdot \text{sec})$ . However, effects do appear for large cone sizes  $R > 0.1$ .

SM segmentation was studied by fixing the strip width at 0.05/8 and looking at the effects of increasing the strip length beyond the EM cell size of 0.05. At standard SSC luminosity, strip lengths of up to 0.4 are benign. At 10 times design luminosity, strips of  $\leq 0.2$  are required.

## REFERENCES

1. D. Green, "Physics Requirements for LHC/SSC Calorimetry" Fermilab-Conf-91/281, Oct. 1991.
2. SDC Calorimeter Conceptual Design Tile/Fiber Scintillator Option Volume I, September 3, 1991.
3. Letter of Intent by the Solenoid Detector Collaboration SDC-91-00151, Nov. 20, 1991. A. Para, et al. "Jet Energy Resolution of the SDC Detector", SDC-90-00149, December 6, 1990.
4. F. Binon, et al. Nucl. Instrum. Methods 206, 373(1983).

5. A. B. Wicklund, "b-Jet Tagging Using Electrons at SDC", SDC-91-00051, Aug. 14, 1991.  
K. Einsweiler, "Associated Higgs Production in the Intermediate Mass Region", SDC-91-00095.  
K. Einsweiler (private communications).
6. J. Freeman and A. Beretvas, Physics of the Superconducting Supercollider, ed. by R. Donaldson and J. Marx (Snowmass, CO 1986) 482.
7. P. Bonamy et al., SDC-90-00153 (Dec. 19, 1990).  
R. Rusack (private communications).

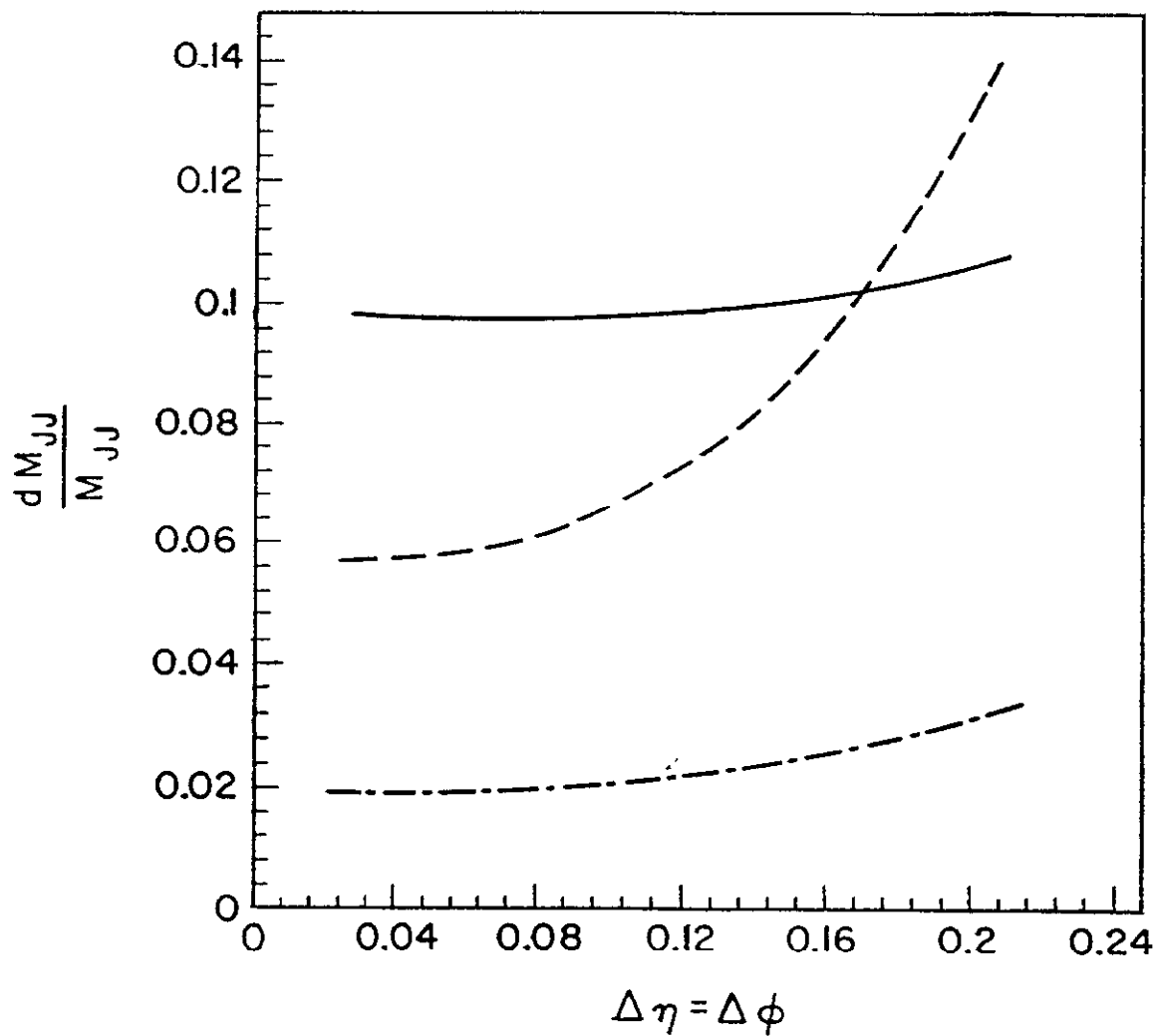


Fig. 1 Dijet mass resolution as a function of the transverse segmentation of the calorimeter cells. The curves are Z with  $P_t = 55$  GeV, solid, Z with  $P_t = 550$  GeV, dashed, and a 10 TeV  $Z'$  produced at low  $P_t$ , dot-dashed.

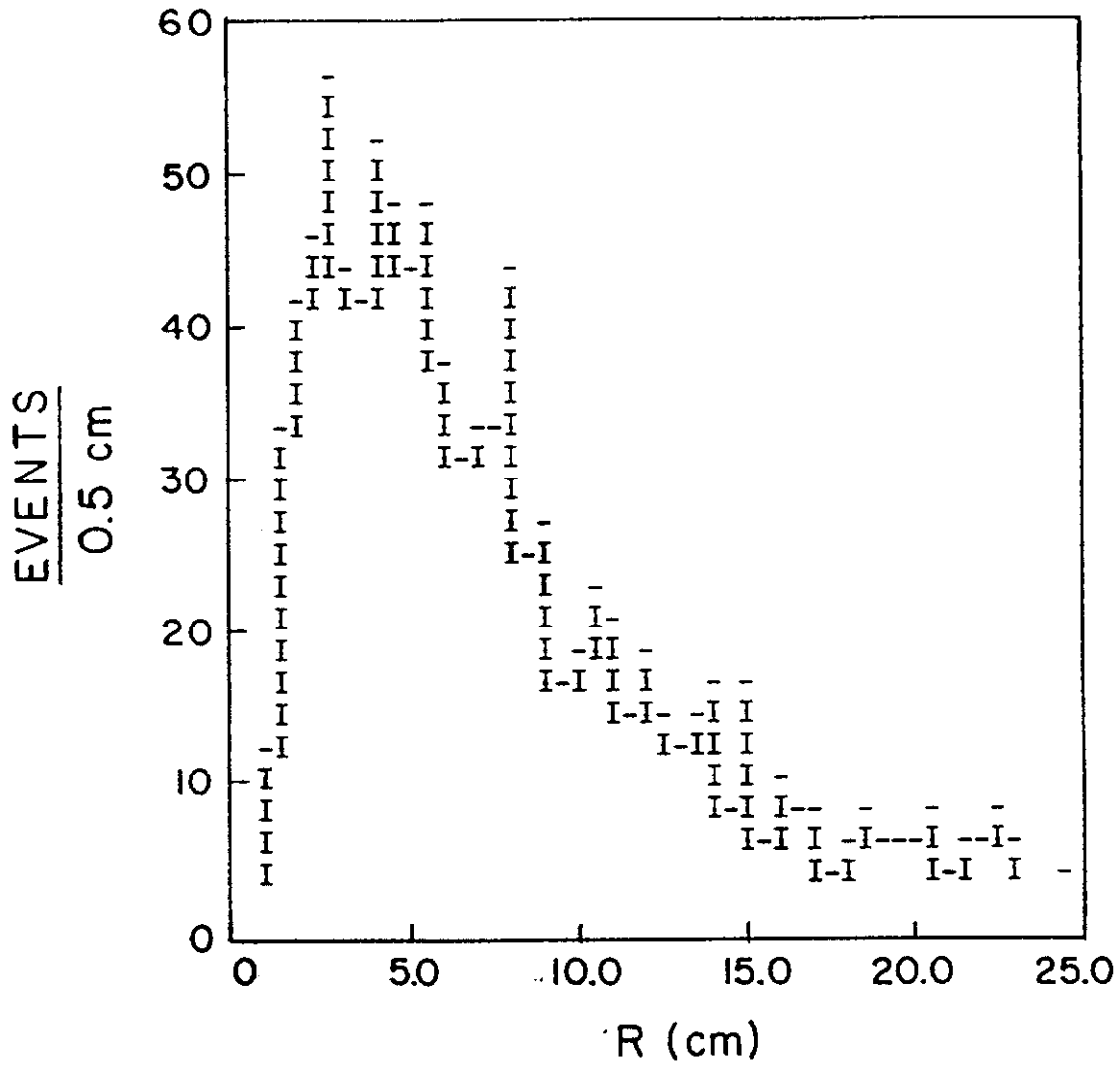


Fig. 2 Radial distribution of an hadronic shower, integrated over all shower depths using the parametrization given in Ref. 4. The mean value of R is,  $\langle R \rangle = 7.5$  cm, with a rms of 5.6 cm.

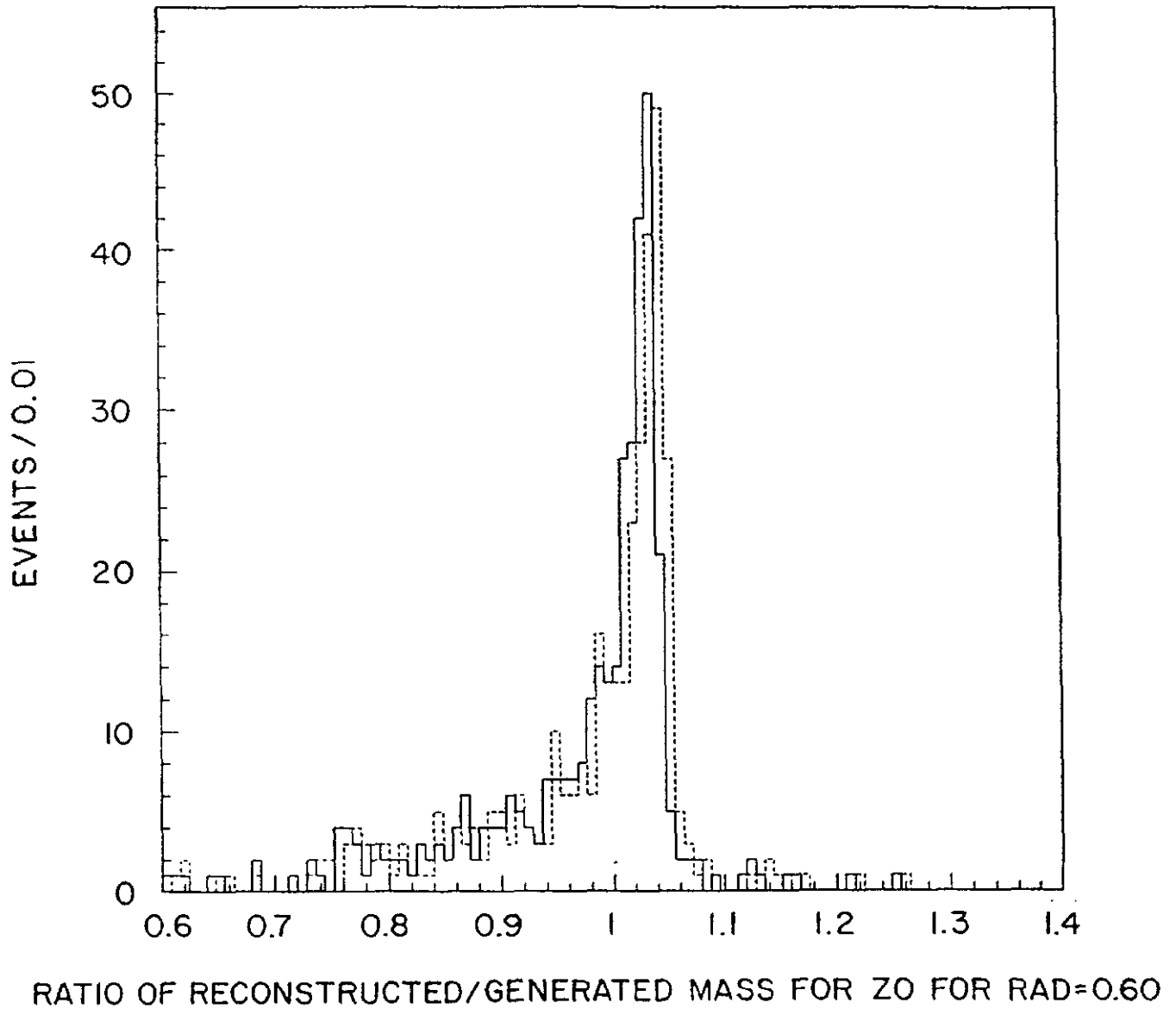


Fig. 3 Histogram of the ratio of reconstructed to generated Z mass with a cluster cone size of  $R = 0.6$ . The EM section has towers of size  $(0.05)^2$  while the HAD towers are  $(0.05)^2$ , solid, and  $(0.1)^2$ , dashed.

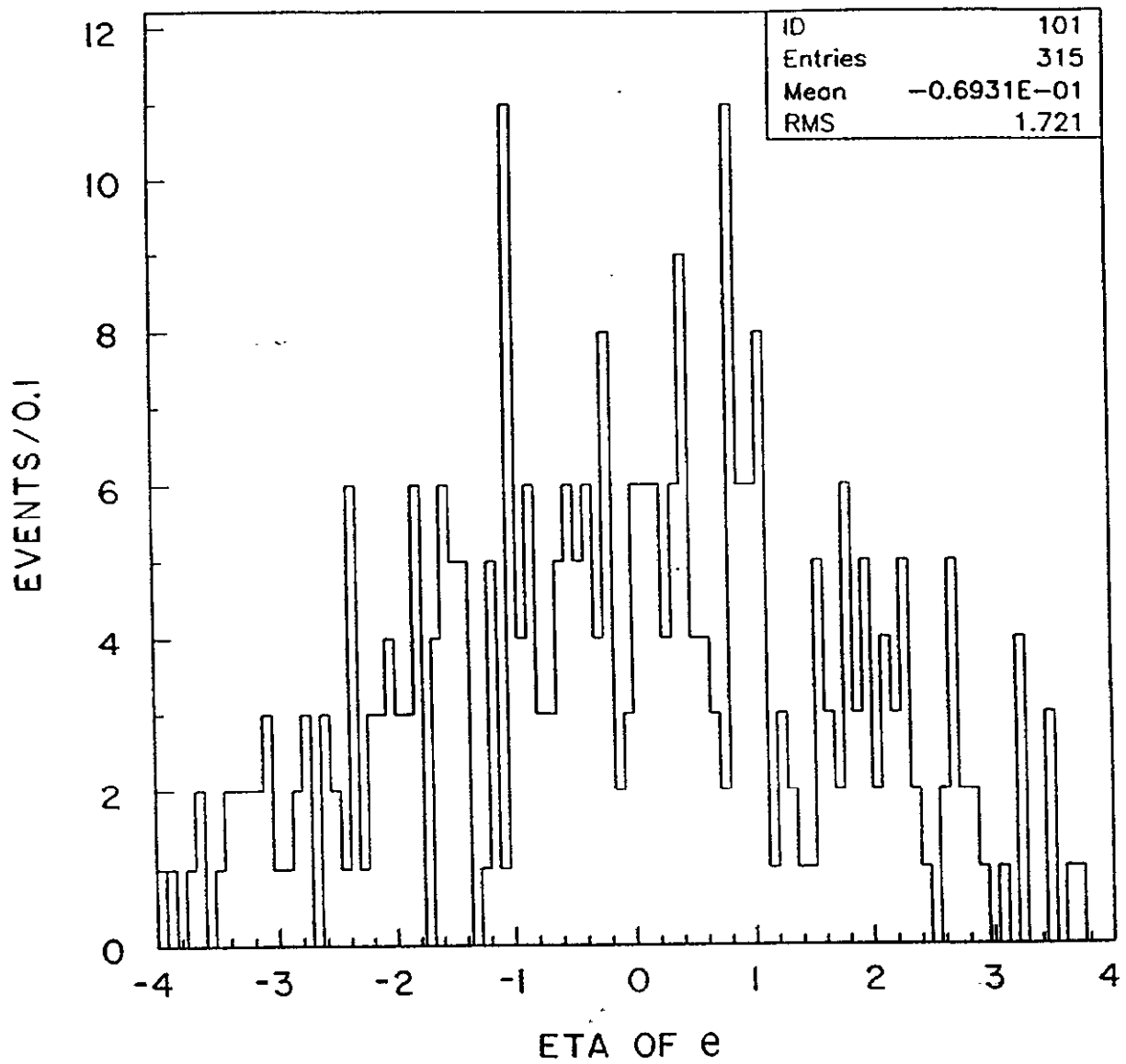


Fig. 4 Histogram of the  $\eta$  distribution of  $e$  from the decays,  $t \rightarrow W + b, b \rightarrow c + e + \nu$ .

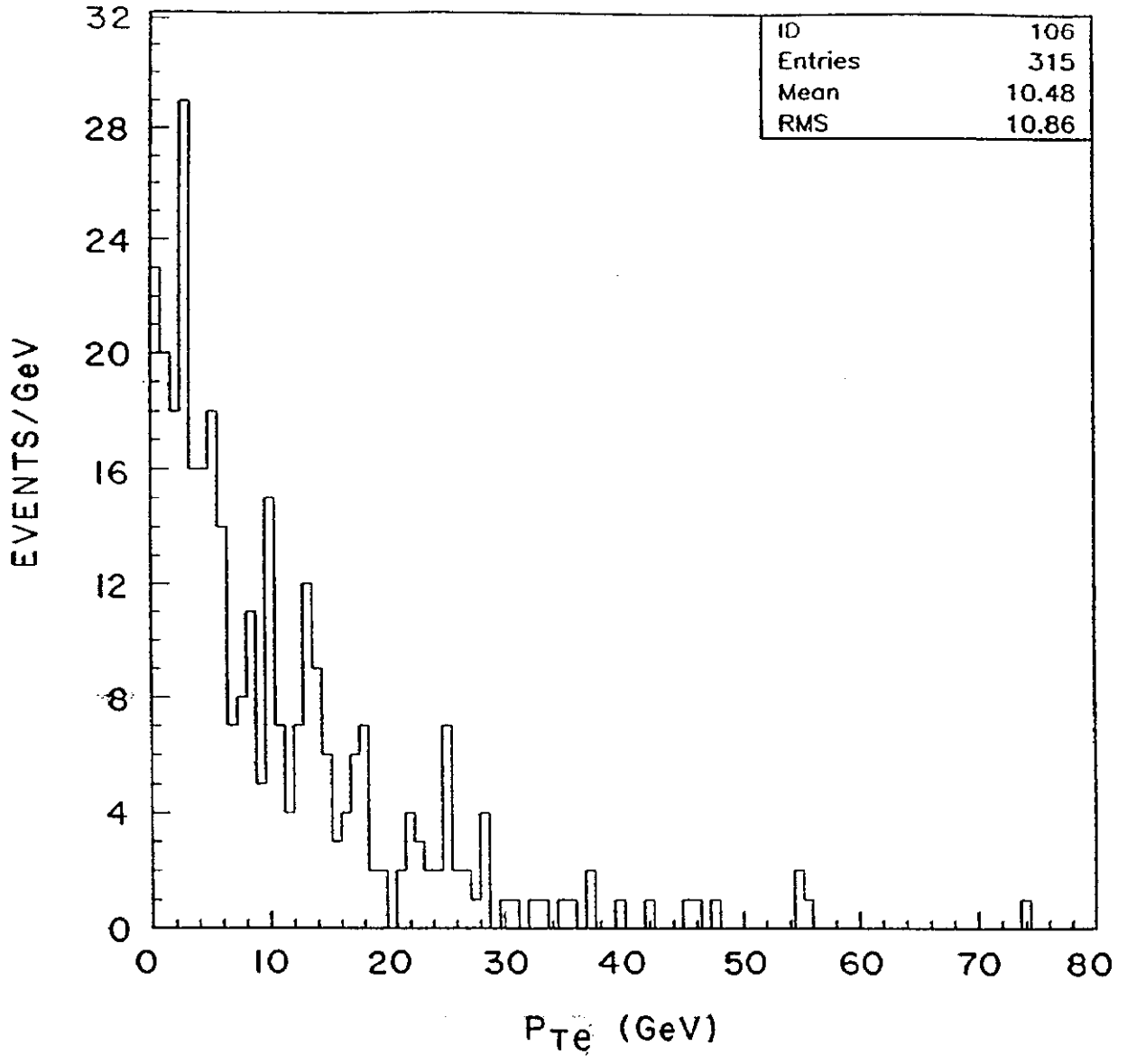


Fig. 5 Histogram of the  $P_T$  distribution of  $e$  from the decays,  $t \rightarrow W + b, b \rightarrow c + e + \nu$ .

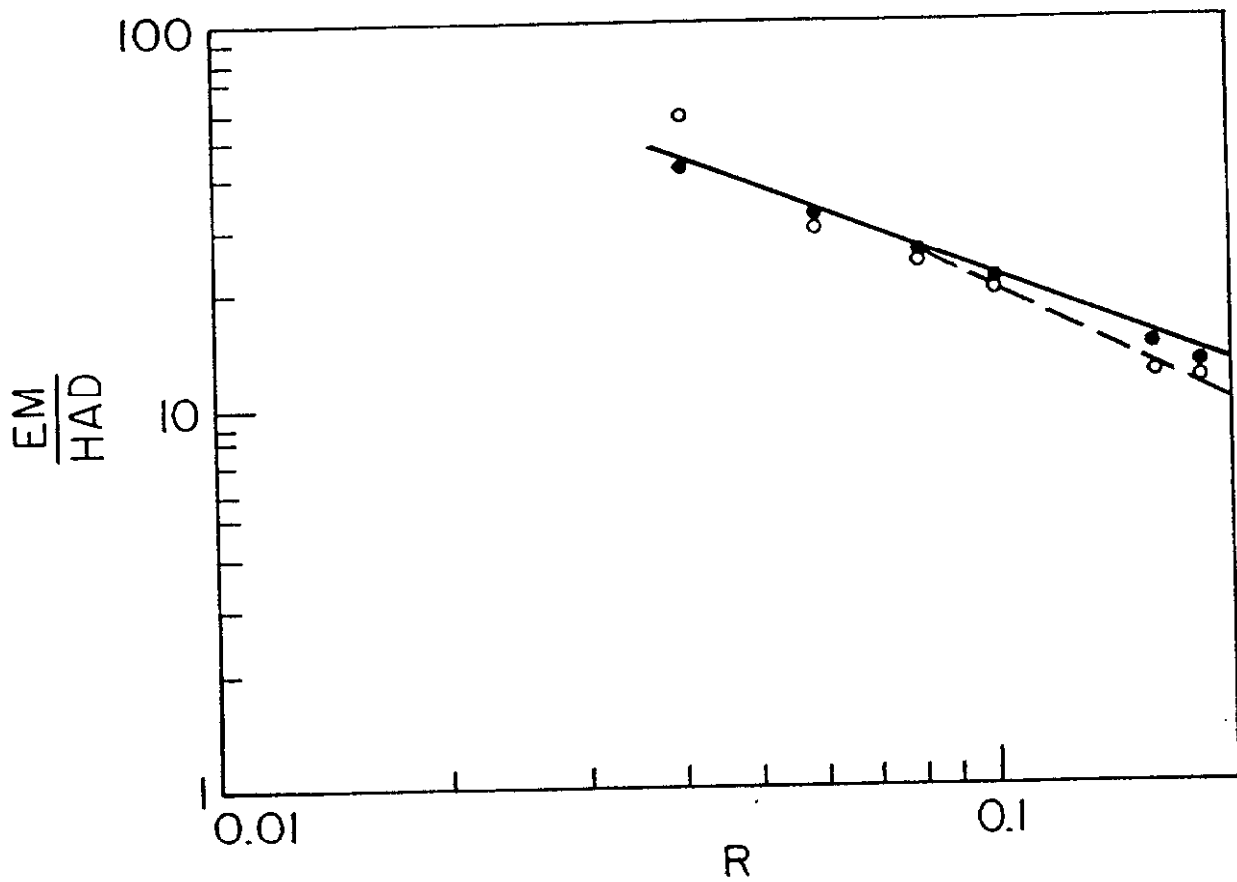


Fig. 6 Plot of the ratio of energy in the EM to the HAD compartment of the calorimetry. The curves refer to EM segmentation of  $(0.05)^2$  and HAD segmentation of  $(0.05)^2$ , solid, and  $(0.1)^2$ , dashed. The radius  $R$  refers to a cone centered on the cell where the maximum  $e$  energy is deposited.

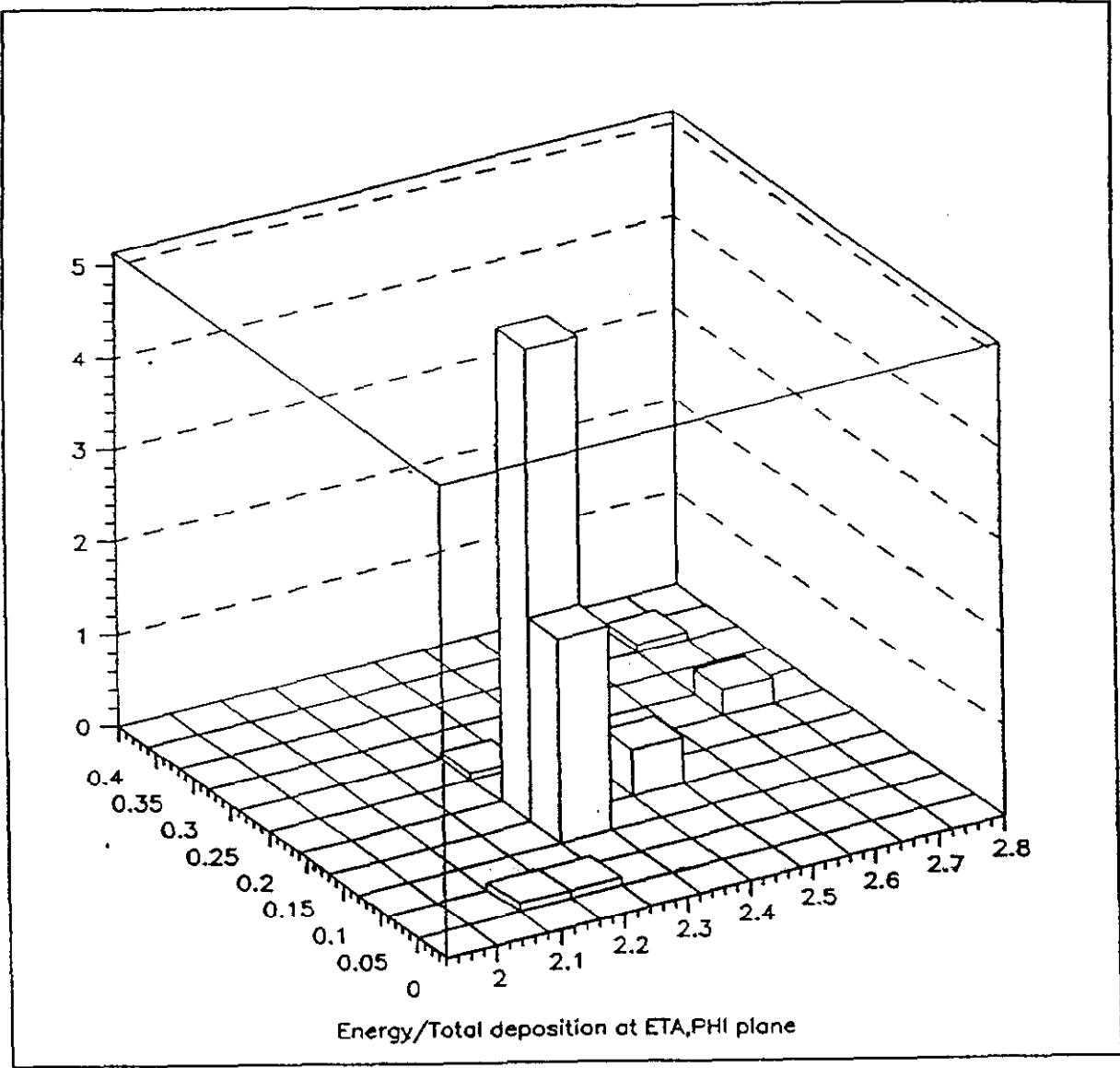


Fig. 7 LEGO plot of the EM+HAD energy deposited near the e cell. The cell size is taken as  $(0.05)^2$ .

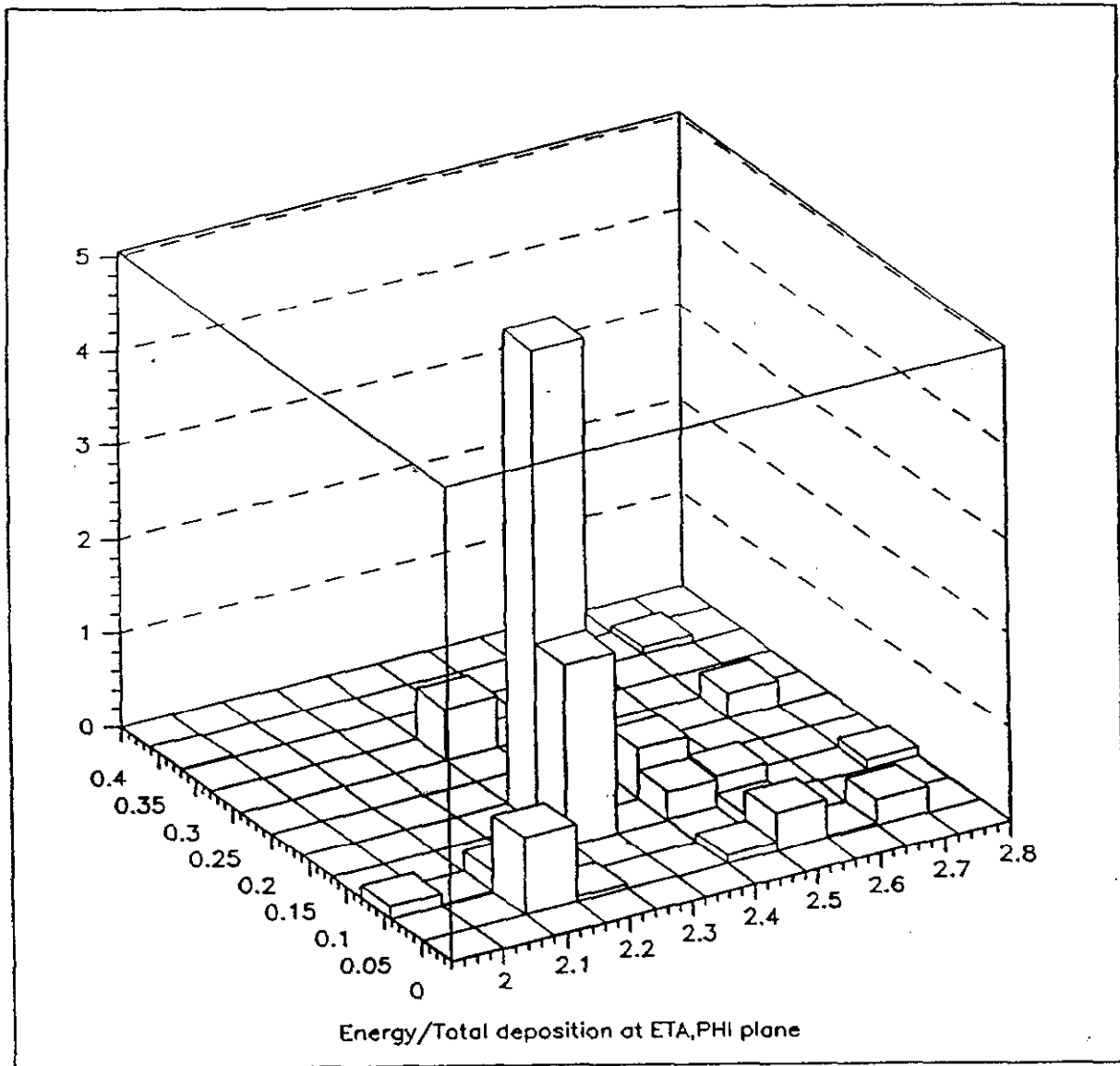


Fig. 8 LEGO plot as in Fig. 7, except that "minbias" events have been overlapped with the  $t\bar{t}$  event. A Poisson distribution with mean of 15 has been assumed for high luminosity operation.

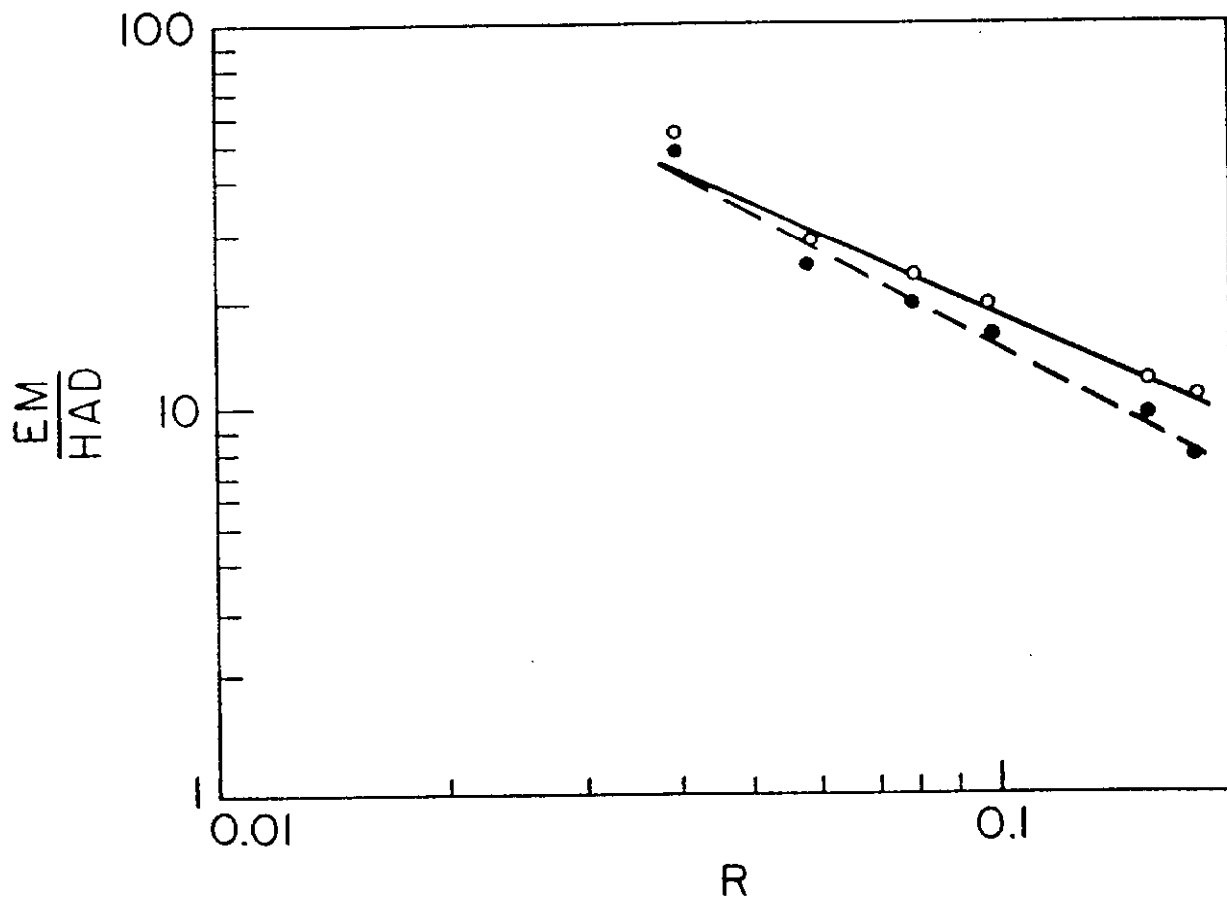


Fig. 9 Plot of EM/HAD as a function of the cluster cone radius for EM cells of size  $(0.05)^2$  and HAD cells of size  $(0.1)^2$ . The solid curve refers to  $\bar{t}\bar{t}$  events alone, while the dashed curve refers to high luminosity operation with a mean of 15 "minbias" events overlapping the  $\bar{t}\bar{t}$  event.

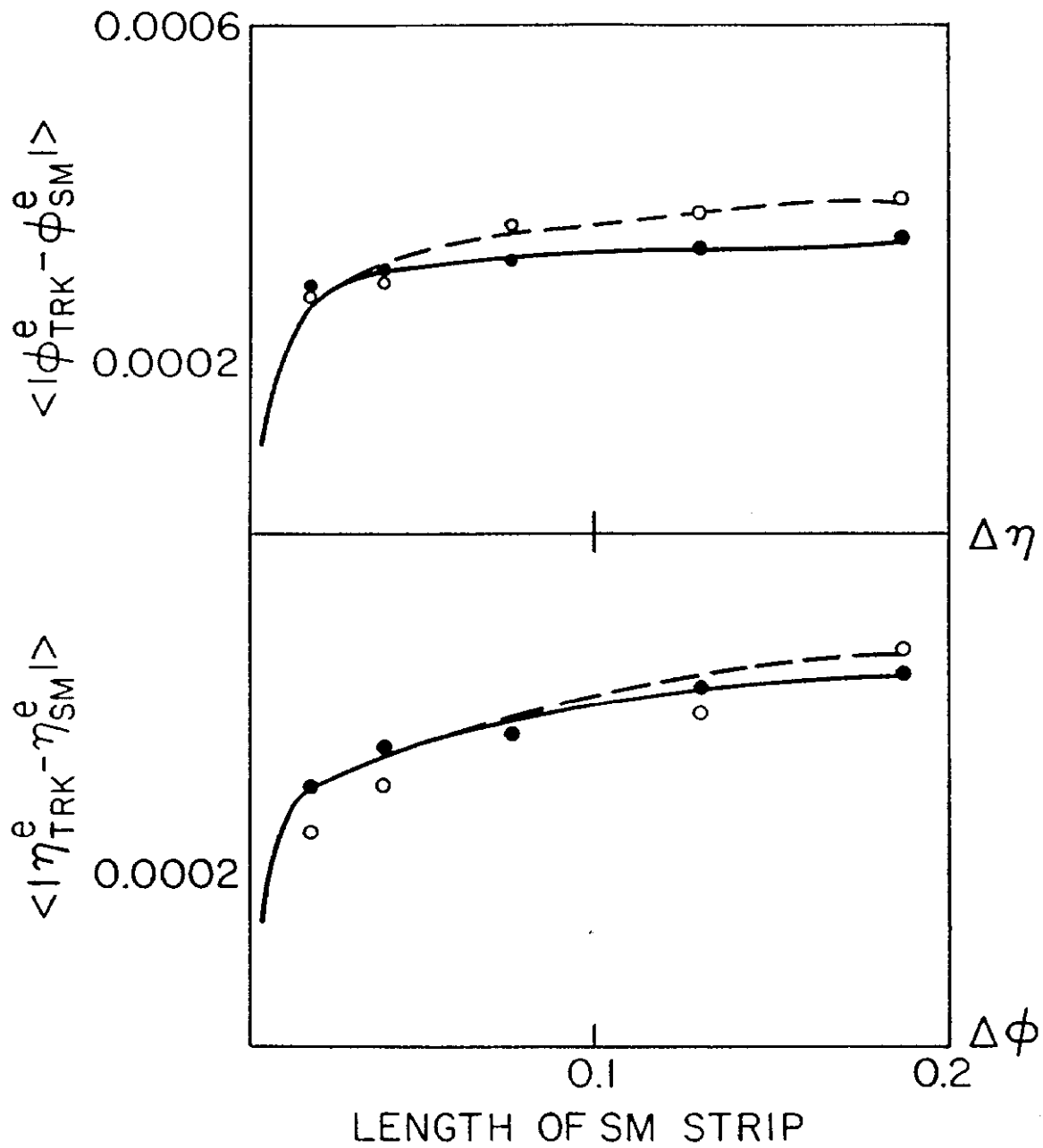


Fig. 10 Plot of the mean deviation of the e track from the energy center of gravity as determined by a Shower Maximum (SM) detector as a function of the strip length. Strips are 0.05/8 wide in  $\eta$  or  $\phi$  (crossed strips). The solid curve refers to  $\bar{t}\bar{t}$  events only. The dashed curve refers to the case where  $\bar{t}\bar{t}$  events have 15 minbias events overlapped.

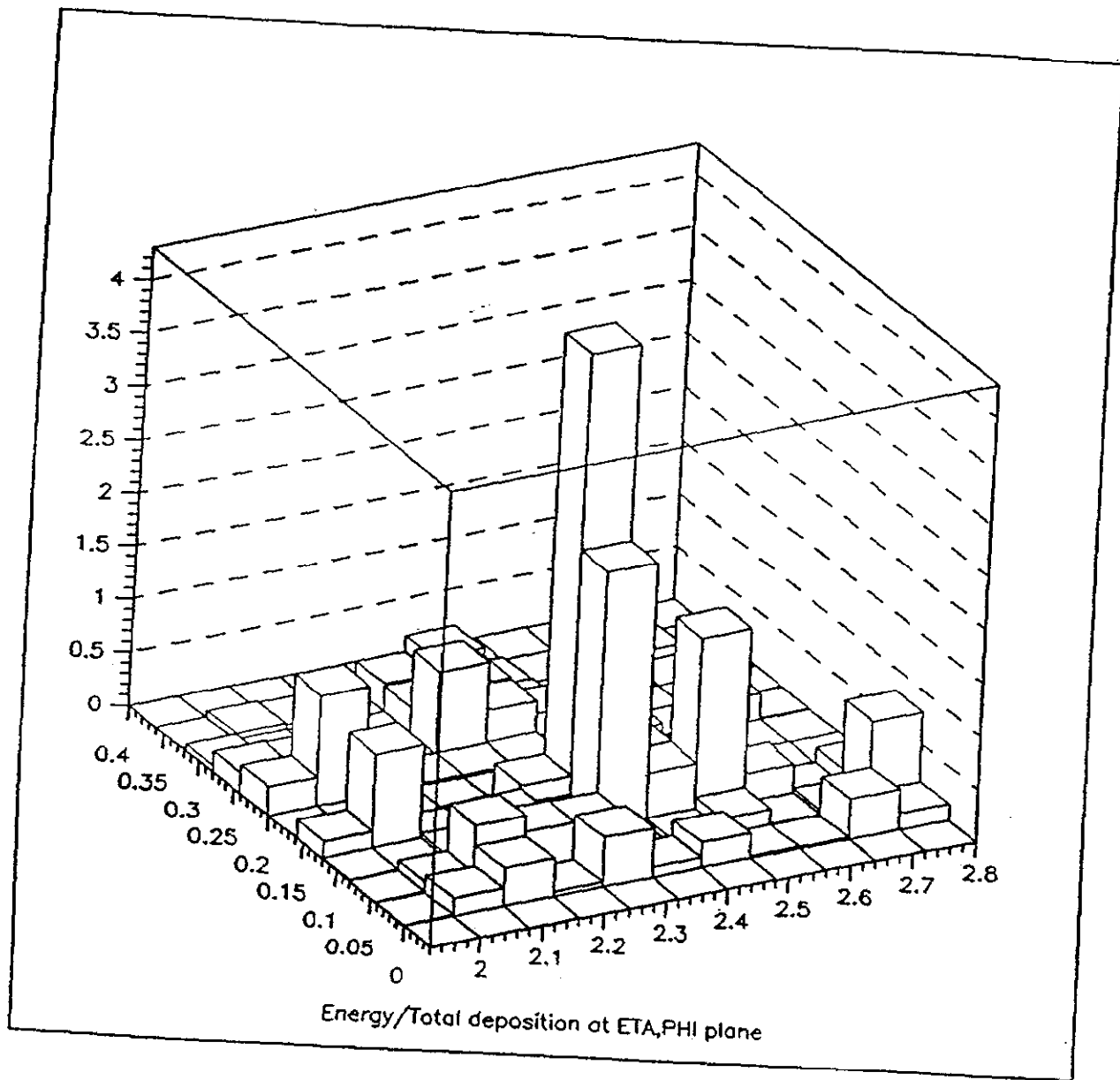


Fig. 11 LEGO plot as in Fig. 8 except the field is turned off. Note, in comparison to Fig. 8, the sweeping effect of the field in removing nearby c fragments.